

## Original Research Article

# Planning feasibility of extremely hypofractionated prostate radiotherapy on a 1.5 T magnetic resonance imaging guided linear accelerator



Mariska D. den Hartogh<sup>a,\*</sup>, Hans C.J. de Boer<sup>a</sup>, Eline N. de Groot-van Breugel<sup>a</sup>, Jochem R.N. van der Voort van Zyp<sup>a</sup>, Jochem Hes<sup>a</sup>, Uulke A. van der Heide<sup>b</sup>, Floris Pos<sup>b</sup>, Karin Haustermans<sup>c</sup>, Tom Depuydt<sup>c</sup>, Robert Jan Smeenk<sup>d</sup>, Martina Kunze-Busch<sup>d</sup>, Bas W. Raaymakers<sup>a</sup>, Linda G.W. Kerkmeijer<sup>a,d</sup>

<sup>a</sup> Department of Radiation Oncology, University Medical Center Utrecht, Utrecht, The Netherlands

<sup>b</sup> Department of Radiation Oncology, The Netherlands Cancer Institute, Amsterdam, The Netherlands

<sup>c</sup> Department of Radiation Oncology, University Hospitals Leuven, Leuven, Belgium

<sup>d</sup> Department of Radiation Oncology, Radboud University Medical Center, Nijmegen, The Netherlands

## ARTICLE INFO

## Keywords:

MRI-linac

Prostate cancer

Stereotactic body radiotherapy

Hypofractionation

Focal boost

## ABSTRACT

**Background and purpose:** Recently, intermediate and high-risk prostate cancer patients have been treated in a multicenter phase II trial with extremely hypofractionated prostate radiotherapy (hypo-FLAME trial). The purpose of the current study was to investigate whether a 1.5 T magnetic resonance imaging guided linear accelerator (MRI-linac) could achieve complex dose distributions of a quality similar to conventional linac state-of-the-art prostate treatments.

**Materials and methods:** The clinically delivered treatment plans of 20 hypo-FLAME patients (volumetric modulated arc therapy, 10 MV, 5 mm leaf width) were included. Prescribed dose to the prostate was  $5 \times 7$  Gy, with a focal tumor boost up to  $5 \times 10$  Gy. MRI-linac treatment plans (intensity modulated radiotherapy, 7 MV, 7 mm leaf width, fixed collimator angle and 1.5 T magnetic field) were calculated. Dose distributions were compared.

**Results:** In both conventional and MRI-linac treatment plans, the V35Gy to the whole prostate was  $> 99\%$  in all patients. Mean dose to the gross tumor volume was 45 Gy for conventional and 44 Gy for MRI-linac plans, respectively. Organ at risk doses were met in the majority of plans, except for a rectal V35Gy constraint, which was exceeded in one patient, by 1 cc, for both modalities. The bladder V32Gy and V28Gy constraints were exceeded in two and one patient respectively, for both modalities.

**Conclusion:** Planning of stereotactic radiotherapy with focal ablative boosting in prostate cancer on a high field MRI-linac is feasible with the current MRI-linac properties, without deterioration of plan quality compared to conventional treatments.

## 1. Introduction

External beam radiotherapy is one of the standard treatment options for clinically localized prostate cancer, and is associated with long-term disease control [1]. For prostate radiotherapy, extreme hypofractionation ( $\geq 5.0$  Gy/fraction), or stereotactic body radiotherapy (SBRT), is increasingly used, as the shortened treatment schedule is more convenient to the patient and potentially cost effective [2,3]. Multiple single arm phase I and II extreme hypofractionation trials, and a recent publication from the HYPO-RT-OC randomized phase II trial using SBRT, showed low rates of severe toxicity and excellent biochemical control for low and intermediate risk prostate cancer patients [4–8].

Given the high fraction dose, highly conformal dose distribution and steep dose gradient seen with SBRT, accurate target volume definition and dose delivery are crucial. The use of multiparametric (mp) magnetic resonance imaging (MRI) has improved target delineation for both the prostate and organs at risk, due to its superior soft-tissue contrast compared to computed tomography (CT) [9–11]. A previous randomized phase III study showed that focal ablative boosting to the mp-MRI visible tumor was feasible and not associated with increased toxicity up to two years after treatment [12].

Prostate targeting accuracy based on position verification using fiducial marker imaging is high [13]. However, treatment of prostate cancer patients on a fully integrated MRI-linac system could increase

\* Corresponding author at: University Medical Center Utrecht, Postbus 85500, 3508 GA Utrecht, The Netherlands.

E-mail address: [m.denhartogh-3@umcutrecht.nl](mailto:m.denhartogh-3@umcutrecht.nl) (M.D. den Hartogh).

<https://doi.org/10.1016/j.phro.2019.07.002>

Received 23 April 2019; Received in revised form 3 July 2019; Accepted 3 July 2019

2405-6316/© 2019 The Authors. Published by Elsevier B.V. on behalf of European Society of Radiotherapy & Oncology. This is an open access article under the CC BY-NC-ND license (<http://creativecommons.org/licenses/by-nc-nd/4.0/>).

treatment precision, further decrease the number of fractions required and omit the need for invasive fiducial marker placement. These MRI-linac systems allow an increased targeting accuracy as variations in daily anatomy and deformations can be fully accounted for by daily contour adjustment and replanning. Moreover, real-time imaging during irradiation offers the potential to characterize and eventually track prostate motion for MRI-guided radiotherapy, dose reconstruction and, ultimately, real-time plan adaptation [14–18]. This could offer the potential for reducing PTV margins, while capturing outliers in intrafractional motion in real time.

Currently, several systems integrating MRI with a linear accelerator or cobalt system are commercially available or being developed [14,19–22]. One of the clinically available systems is a high field (1.5 Tesla (T)) MRI-linac system, which has some technical differences compared to standard clinical linacs (e.g. a fixed collimator angle, larger leaf width, 7 MV intensity modulated radiotherapy (IMRT) delivery only) [23]. Furthermore, the presence of a 1.5 T magnetic field potentially may affect the dose distribution, e.g. due to the electron return effect [24]. This effect is observed at boundaries between tissues with large density differences and can induce an increase in local dose, mainly when a single photon beam would be used. For MRI-guided prostate radiotherapy this could particularly affect the dose distribution near rectal air pockets. The present study is an R-IDEAL stage 0 study in preparation of the clinical implementation of MRI-linac treatment for prostate cancer [25]. R-IDEAL is a framework for systematic evaluation and implementation of technical innovations in medical practice. Stage 0 studies include all preparations required before a technical innovation can be clinically introduced.

The purpose of this study was to investigate whether a 1.5 T MRI-linac system could achieve dose distributions of a quality similar to conventional state-of-the-art prostate treatments in patients who are treated with stereotactic whole prostate radiotherapy with focal ablative dose escalation to the visible tumor.

## 2. Materials and methods

### 2.1. Patients

The present planning study involved 20 randomly selected clinically delivered treatment plans from patients treated within the hypo-FLAME study at the University Medical Center Utrecht. The hypo-FLAME study was approved by the institutional review board and the informed consent included approval to use the acquired data for future studies. This study is a multicenter phase II study performed at the UMC Utrecht, NKI-AvL Amsterdam, Radboudumc Nijmegen (The Netherlands) and UZ Leuven (Belgium), which recently completed inclusion ( $n = 100$ ). The main objective is to determine whether administering a focal simultaneously integrated SBRT boost (up to 50 Gy in 5 weekly fractions) to the MRI-defined macroscopic tumor volume, in addition to whole gland prostate SBRT (35 Gy), is clinically feasible and associated with acceptable toxicity. For more information on the hypo-FLAME study, see the Clinical Trials Registry (NCT02853110).

### 2.2. Radiotherapy simulation and contouring

Before radiotherapy treatment, gold fiducial markers were inserted and a multiparametric (mp) MRI (T2 weighted, diffusion weighted imaging (DWI) and dynamic contrast enhanced (DCE) sequences) and radiotherapy planning CT scan were performed. Patients were planned and treated in supine position. Patients were advised to have a comfortably full bladder prior to radiotherapy planning and each treatment fraction. The MRI protocol is consistent with European Society of Urogenital Radiology (ESUR) guidelines [26]. The planning CT scan was registered with the MRI.

The tumor nodules as visible on mpMRI were contoured as gross tumor volume (GTV). In five patients, two separate GTVs were

contoured and planned for both planning modalities, resulting in 25 GTVs eligible for analysis. The whole prostate gland was considered clinical target volume (CTV; including the GTV + 4 mm margin, excluding organs at risk). The seminal vesicles were contoured at the discretion of the treating physician. The margin from the CTV contour around the prostate to planned target volume (PTV) was 4 mm based on earlier experience with volumetric modulated arc therapy (VMAT) prostate SBRT [27]. The rectum was contoured from the external sphincter of the anus to the rectosigmoid flexure, the anal canal was contoured from the external sphincter up to the internal sphincter (typically 3 cm). The penile bulb, prostatic urethra and the bladder were also delineated. The small bowel was only contoured when located near the PTV.

### 2.3. Treatment planning and dose constraints

MRI-linac plans were created for the Unity linac (Elekta AB) which integrates a 1.5 T MR scanner with a 7 MV linac mounted on a ring gantry. Beam characteristics and the presence of a magnetic field and cryostat were all accounted for in the treatment planning software. In order to fully account for the influence of the electron-return-effect in case of rectal gas, no density override was applied to the rectum in the MRI-linac treatment plans. Beam characteristics are described in detail by Woodings et al. and first patient treatments were performed in May 2017 [14,28]. The most important differences of the MRI-linac system compared to our conventional linac are (1) the 1.5 T magnetic field, (2) the 7 mm leaf width at isocenter, (3) the fixed collimator angle with leaves traveling in craniocaudal direction, (4) the 7 MV flattening filter free beam energy, (5) the cryostat and body-coil the beam needs to pass, (6) the fixed table top to isocenter distance of 13 cm and (7) the step-and-shoot IMRT delivery. Therefore, it was not a priori evident that dose distributions on the MRI-linac could match those on the conventional machines.

The MRI-linac IMRT plans were created in the clinically commissioned Monaco TPS (v5.19) using a 7 beam setup. The minimum segment area and width were 1.5 cm<sup>2</sup> and 0.5 cm, respectively. The minimum number of monitor units per segment was 5, with a maximum of 125 segments. The calculation grid spacing was 3 mm with a statistical dose uncertainty per control point of 3% and < 1% per voxel. Patients were treated on conventional Agility linacs (5 mm MLC leaf width) using 10 MV VMAT plans, dual full arc, created in the Monaco TPS (Elekta AB). The maximum number of control points per arc was 144. The minimum segment width was 0.5 cm. The grid spacing was 3 mm, with a statistical uncertainty per control point of 8% and < 1% per voxel. Dose to medium was applied for both planning techniques.

For comparison of the Agility linac and MRI-linac plans, dose–volume histograms (DVHs) for all volumes of interest and corresponding dose parameters were calculated. Planning constraints for coverage of the target volumes and organs at risk (OAR) are depicted in Table 1. OAR constraints were based on the pHART6 and 7 studies with additional dose constraints added by the hypo-FLAME study group [29]. Not exceeding OAR constraints was considered of higher importance than boosting the GTV, therefore, GTV doses were as high as achievable (up to 50 Gy) while respecting the OAR constraints (iso-toxic boosting).

### 2.4. Data analysis

MRI-linac dose distributions were compared to those of the corresponding clinically delivered conventional treatment plans. Median values on coverage, high dose volumes and OAR doses were evaluated. Non-parametric testing was performed to compare the paired variables by performing a Wilcoxon signed-rank test by using IBM SPSS Statistics 20 (Chicago, IL, USA) with a significance level of  $\alpha$  below 0.05.

**Table 1**  
Target volume dose prescription and OAR constraints for the hypo-FLAME study.

<b>Target coverage</b>	
GTV_5000	V40Gy > 99% (if possible) Dmax V52Gy (if possible)
CTV_3500	V35Gy > 99%
PTV_3325	V33.25 Gy > 99%
PTV_3000	V30Gy > 99%
<b>OAR constraints</b>	
Rectum	Dmax < 40 Gy V35Gy 2 cc (if possible < 1 cc) V32Gy ≤ 15% V28Gy ≤ 20%
Rectum_PRV2mm*	Dmax < 42 Gy
Bladder	V42Gy < 1 cc V37Gy < 5 cc V32Gy ≤ 15% V28Gy ≤ 20%
Urethra	Dmax < 42 Gy
Urethra_PRV2mm*	Dmax < 42 Gy
Small bowel#	Dmax < 35 Gy V19.5 < 5 cc
Penile bulb	V20Gy ≤ 90%
Femoral head	V28Gy ≤ 5%

Dose constraints pHART studies and hypo-FLAME group \* Planned risk volume (PRV) # Only contoured when adjacent to PTV.

### 3. Results

Comparable treatment plans for stereotactic prostate radiotherapy with focal ablative boosting could be created for the conventional linac and MRI-linac. The dose as prescribed to the whole prostate gland was adequately covered for both treatment modalities (Table 2). Regarding the GTV boost, the median V40Gy was > 99% for both planning modalities. The corresponding median dose to the GTV boost was 45 Gy

(range 43–51) for conventional plans and 44 Gy (range 42–49 Gy) for MRI-linac plans, respectively. The V52Gy (104%) was exceeded in two patients on conventional plans by 1 cc at most. In MRI-linac plans, V52 Gy was 0.2 cc in one patient. OAR constraints were not exceeded in these particular patients. For the rectum, bladder, urethra and bowel, no clinically relevant differences in median dose constraints were observed between planning modalities, although some differences were statistically significant. For rectal dose, the V35Gy was exceeded in one conventionally planned patient by 1.2 cc and for the MRI-linac plan by 0.6 cc. In one other patient, the V32Gy for the bladder was slightly exceeded by 3% for the MRI-linac plan, but not for the conventional plan. For a patient with a Bricker deviation and a native (empty) bladder in situ, the V32Gy and V28Gy for the native bladder were exceeded by 11% and 17% respectively for the conventional plan and 14% and 19% for the MRI-linac plan, which was clinically accepted. For another patient the penile bulb dose was exceeded for both modalities, which was clinically accepted. Fig. 1 shows a sagittal view of a conventional and MRI-linac treatment plan for a hypo-FLAME patient with a large amount of rectal air.

The average number of monitor units and segments was 2970 and 226 for conventional VMAT plans and 2975 and 120 for MRI linac IMRT plans, respectively.

### 4. Discussion

The results of this study show that stereotactic treatment planning with an ablative tumor boost in prostate cancer on a high field MRI-linac is comparable to conventional VMAT treatment planning in terms of dose parameters. In one patient, one bladder constraint (V32Gy) was exceeded slightly for the MRI-linac plan and not for the conventional plan. For the other OAR exceeding's, the constraints were exceeded for both planning modalities. As these particular constraints were challenging to meet for both planning techniques, constraint violation was not considered the result of differences in planning properties or the use of either an IMRT or VMAT technique but due to the challenge of SBRT with focal boost planning in general. Therefore, no clinically relevant

**Table 2**  
Dosimetric parameters for conventional and MRI-linac treatment plans.

		Conventional VMAT		MRI-linac IMRT		p value
		median	range	median	range	
<b>Target coverage</b>						
GTV_5000	V40Gy (%)	99.8	97.5–100	99.9	97.7–100	0.41
	V52Gy (cc)	0.0	0.0–1.1	0.0	0.0–0.2	0.07
	Mean dose (Gy)	45.1	43.34–50.6	44.1	42.31–48.6	< 0.01
CTV_3500	V35Gy (%)	99.9	99.4–100	99.9	99.2–100	0.60
PTV_3325	V33.25 Gy (%)	99.1	98.2–99.8	99.7	98.7–100	< 0.01
PTV_3000	V30Gy (%)	99.1	98.5–100	99.9	99.6–100	< 0.01
<b>OAR constraints</b>						
Rectum	Dmax (Gy)	37.7	35.90–40.9	36.9	36.0–41.2	0.04
	V35Gy (cc)	1.0	0.1–3.2	0.8	0.1–2.6	< 0.01
	V32Gy (%)	5.0	2.7–7.5	4.8	2.9–9.2	0.94
	V28Gy (%)	10.4	6.1–17.0	9.9	5.3–16.0	0.88
Rectum_PRV2mm	Dmax (Gy)	40.4	37.10–42.2	39.1	37.1–42.0	0.02
Bladder	V42Gy (cc)	0.0	0.0–0.2	0.0	0.0–0.4	0.44
	V37Gy (cc)	1.5	0.0–4.9	0.4	0.0–5.0	0.17
	V32Gy (%)	7.1	2.1–26.0	8.3	2.1–28.9	< 0.01
	V28Gy (%)	11.0	4.9–37	12.5	4.7–39.3	< 0.01
Urethra	Dmax (Gy)	40.5	38.6–41.2	40.4	38.4–41.7	0.41
Urethra_PRV2mm	Dmax (Gy)	41.8	41.3–42.1	41.8	40.7–42.6	0.55
Bowel	Dmax (Gy)	1.7	0.7–12.8	2.7	1.3–11.2	0.03
	V19.5 (cc)	0.0	0.0	0.0	0.0	
Penile bulb	V20Gy (%)	5.4	0–97.3	12.7	0–100	< 0.01
Femoral heads	V28 (%)	0.0	0.0–0.0	0.0	0.0–0.0	

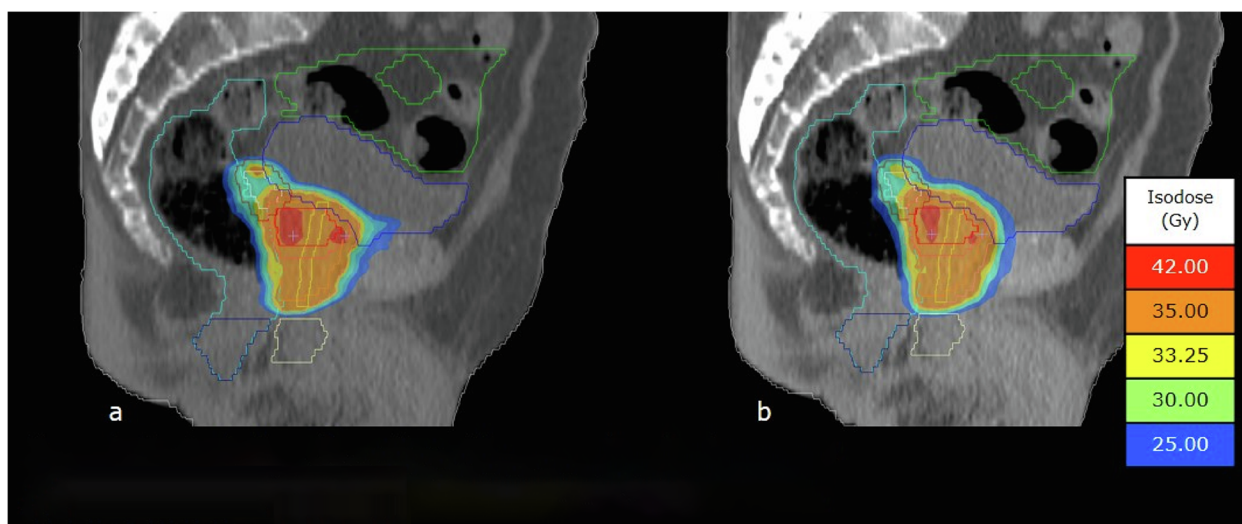


**Fig. 1.** Sagittal view of a patient with air pockets in the rectum (a) VMAT plan on a conventional linac (b) IMRT plan on an MRI-linac. Delineated target structures: pink PTV\_3325, red GTV\_5000, white CTV\_3000, brown PTV\_3000. Delineated organs at risk: light blue rectum with anal canal, dark blue bladder, green small bowel, yellow urethra, white penile bulb. (For interpretation of the references to colour in this figure legend, the reader is referred to the web version of this article.)

influences of the larger leaf width, 7 MV IMRT technique or electron-return-effect in MRI-linac treatment plans were observed.

As SBRT with focal boost treatment planning on a high field MRI-linac is feasible for prostate cancer, it allows further exploitation of possible advantages of adaptive radiotherapy on the current clinical high field MRI-linac machine. Its fundamental assets are both daily and continuous intrafraction soft tissue imaging [14,30]. Daily MRI can be used for soft-tissue based position verification or for contour adjustment and replanning [23]. Real-time imaging during irradiation, combined with future options for active motion compensation like gating or even online dose reconstruction and real-time plan adaptation, offers the potential for future PTV margin reduction and OAR sparing [14–18]. This could eventually allow for further hypofractionation in prostate radiotherapy.

In this study, an identical 5 mm PTV margin was used for both conventional VMAT and MRI-linac treatment plans. As the dose rate of the MRI-linac is lower than on our conventional linacs (420 vs. 600 MU/min), and IMRT is used instead of VMAT, the treatment times on an MRI-linac will be longer. This might have a substantial effect on intrafractional motion, which could acquire PTV margin adjustments. For this study, in which the purpose was only to investigate the influence of the magnetic field on treatment planning, PTV margins were deliberately kept identical. Moreover, with the future MRI-linac possibilities for online motion compensation and replanning, as described above, the intrafractional motion during the prolonged treatment time can be actively compensated for. However, before performing stereotactic prostate radiotherapy on the MRI-linac, dealing with intrafraction motion based on cine MRI needs to be further developed [31].

In addition to beam-on time, the total duration of a treatment session on the current MRI-linac can be substantially longer than on a regular linac. The different stages during an MRI-linac treatment session using a so-called ‘adapt to shape’ workflow consist of MRI-acquisition, image registration, contour propagation and adjustment, replanning, acquisition of a second MRI for position verification, dose check, radiotherapy delivery and intrafraction- and post-treatment MRI acquisition [14,23,32]. Treatment session times of clinically delivered MRI-linac treatments in patients with lymph node metastases were typically within 60 min, which we also would expect for prostate SBRT [32]. Future treatment session times are expected to decrease, as they are subject to experience and technical developments like shorter computational times with increasing computer power, smarter algorithms, even faster MRI, and improved contour propagation.

The purpose of this study was to evaluate the effect of the magnetic field on radiotherapy treatment planning. As the electron return effect is particularly evident at air-tissue boundaries, no density override to the rectum was applied, to fully account for the effect of rectal gas pockets. Air cavities can appear or disappear during irradiation. The effect of intrafractional nonstationary spherical air cavities, within a target volume, on IMRT dose delivery in the presence of a magnetic field was studied in a phantom study by Bol et al. [33]. They found single voxel dose differences up to 5%. These findings were confirmed by a MRI-linac planning study in rectal cancer patients by Uilkema et al. [34]. Both of these studies investigated air cavities within the target volume and not adjacent to the target, as will be the case in prostate cancer treatment. However, MRI-guidance during treatment would allow for detection of air cavity changes and adaptive strategies.

The time spent on pre-treatment treatment planning was not measured. Treatment planning time for MRI-linac was prone to a learning curve and is highly dependent on the calculation power of the hardware. In our current clinical practice, MRI-linac plans can be derived within a time frame comparable to clinical VMAT treatment plans.

This was the first study investigating plan equivalency between conventional and high field MRI-linac treatment plans for extremely hypofractionated prostate cancer radiotherapy with a focal boost. Our findings are in line with studies investigating this effect in conventional or moderately hypofractionated prostate radiotherapy [35–37]. Also for other tumor sites, as lung, (partial) breast, rectum and pancreas, the influence of the magnetic field has been evaluated and resulted in small dose differences and clinically acceptable plans [34,35,38–43].

A strength of the study is that the data of 20 clinically delivered VMAT SBRT treatment plans from the hypo-FLAME study were used. Consequently, clinically derived contours and clinically applied constraints of target volumes and OARs were used to create MRI-linac treatment plans. In this study, IMRT plans were compared to VMAT plans. This difference in technique was accepted deliberately as the purpose of the study was to investigate plan equivalency between MRI-linac (which offers step-and-shoot IMRT) and the current standard of care in our institute (which is VMAT).

Additional studies have been initiated to determine the effect of online adaptive planning on the MRI-linac on target coverage and OAR dose and, subsequently, on biochemical disease free survival and toxicity. Multicenter MRI-guided feasibility studies in an international research consortium have started using a 1.5 T MRI-linac for prostate cancer patients and MRI-guided treatment will continuously be



improved within the context of the R-IDEAL framework.

In conclusion, planning of stereotactic ablative focal boosting in prostate cancer on a high field MRI-linac is feasible, without deterioration of plan quality compared to treatment on a conventional linac.

### Conflict of interest

The MRI-linac scientific consortium is partly funded by Elekta AB (Stockholm, Sweden) and Philips Medical Systems (Best, The Netherlands). The University Medical Center Utrecht, The Netherlands Cancer Institute and the Radboudumc are members of this consortium. The authors from the UZ Leuven wish to confirm that there are no known conflicts of interest associated with this publication. There has been no financial support for this work in particular.

### Appendix A. Supplementary data

Supplementary data to this article can be found online at <https://doi.org/10.1016/j.phro.2019.07.002>.

### References

- [1] Hamdy FC, Donovan JL, Lane JA, Mason M, Metcalfe C, Holding P, et al. 10-Year outcomes after monitoring, surgery, or radiotherapy for localized prostate cancer. *N Engl J Med* 2016;375:1415–24.
- [2] Pan HY, Jiang J, Hoffman KE, Tang C, Choi SL, Nguyen QN, et al. Comparative toxicities and cost of intensity-modulated radiotherapy, proton radiation, and stereotactic body radiotherapy among younger men with prostate cancer. *J Clin Oncol* 2018;36:1823–30.
- [3] Zietman AL. Making radiation therapy for prostate cancer more economical and more convenient. *JCO* 2016;34:2323–4.
- [4] Kishan AU, Dang A, Katz AJ, Mantz CA, Collins SP, Aghdam N, et al. Long-term outcomes of stereotactic body radiotherapy for low-risk and intermediate-risk prostate cancer. *JAMA Netw Open* 2019;2:e188006.
- [5] Kothari G, Loblaw A, Tree AC, van As NJ, Moghanaki D, Lo SS, et al. Stereotactic body radiotherapy for primary prostate cancer. *Technol Cancer Res Treat* 2018;17:1533033818789633.
- [6] Katz A. Stereotactic body radiotherapy for low-risk prostate cancer: a ten-year analysis. *Cureus* 2017;9:e1668.
- [7] Widmark A, Gunnlaugsson A, Beckman L, Thellenberg-Karlsson C, Hoyer M, Lagerlund M, et al. Extreme hypofractionation versus conventionally fractionated radiotherapy for intermediate risk prostate cancer: early toxicity results from the Scandinavian randomized phase III trial “HYPO-RT-PC. *Int J Radiat Oncol Biol Phys* 2016;96:938–9.
- [8] Widmark A, Gunnlaugsson A, Beckman L, Thellenberg-Karlsson C, Hoyer M, Lagerlund M, et al. Ultra-hypofractionated versus conventionally fractionated radiotherapy for prostate cancer: 5-year outcomes of the HYPO-RT-PC randomised, non-inferiority, phase 3 trial. *Lancet* 2019. [https://doi.org/10.1016/S0140-6736\(19\)31131-6](https://doi.org/10.1016/S0140-6736(19)31131-6).
- [9] Rasch C, Barillot I, Remeijer P, Touw A, van Herk M, Lebesque JV. Definition of the prostate in CT and MRI: a multi-observer study. *Int J Radiat Oncol Biol Phys* 1999;43:57–66.
- [10] Smith WL, Lewis C, Bauman G, Rodrigues G, D'Souza D, Ash R, et al. Prostate volume contouring: a 3D analysis of segmentation using 3DTRUS, CT, and MR. *Int J Radiat Oncol Biol Phys* 2007;67:1238–47.
- [11] Sander L, Langkilde NC, Holmberg M, Carl J. MRI target delineation may reduce long-term toxicity after prostate radiotherapy. *Acta Oncol* 2014;53:809–14.
- [12] Monnikhof EM, van Loon JWL, van Vulpen M, Kerkmeijer LGW, Pos FJ, Hausermans K, et al. Standard whole prostate gland radiotherapy with and without lesion boost in prostate cancer: toxicity in the FLAME randomized controlled trial. *Radiother Oncol* 2018;127:74–80.
- [13] Mutanga TF, de Boer HC, van der Wielen GJ, Wentzler D, Barnhoorn J, Incrocci L, et al. Stereographic targeting in prostate radiotherapy: speed and precision by daily automatic positioning corrections using kilovoltage/megavoltage image pairs. *Int J Radiat Oncol Biol Phys* 2008;71:1074–83.
- [14] Raaymakers BW, Jurgensliemk-Schulz IM, Bol GH, Glitzner M, Kotte ANTJ, van Asselen B, et al. First patients treated with a 1.5 T MRI-Linac: clinical proof of concept of a high-precision, high-field MRI guided radiotherapy treatment. *Phys Med Biol* 2017;62:L41–50.
- [15] Stemkens B, Tijssen RH, de Senneville BD, Lagendijk JJ, van den Berg CA. Image-driven, model-based 3D abdominal motion estimation for MR-guided radiotherapy. *Phys Med Biol* 2016;61:5335–55.
- [16] Kontaxis C, Bol GH, Stemkens B, Glitzner M, Prins FM, Kerkmeijer LGW, et al. Towards fast online intrafraction replanning for free-breathing stereotactic body radiation therapy with the MR-linac. *Phys Med Biol* 2017;62:7233–48.
- [17] Dietz B, Yip E, Yun J, Fallone BG, Wachowicz K. Real-time dynamic MR image reconstruction using compressed sensing and principal component analysis (CS-PCA): demonstration in lung tumor tracking. *Med Phys* 2017;44:3978–89.
- [18] Glitzner M, Crijns SP, de Senneville BD, Kontaxis C, Prins FM, Lagendijk JJ, et al. On-line MR imaging for dose validation of abdominal radiotherapy. *Phys Med Biol* 2015;60:8869–83.
- [19] Raaymakers BW, Lagendijk JJ, Overweg J, Kok JG, Raaijmakers AJ, Kerkhof EM, et al. Integrating a 1.5 T MRI scanner with a 6 MV accelerator: proof of concept. *Phys Med Biol* 2009;54:N229–37.
- [20] Mutic S, Dempsey JF. The ViewRay system: magnetic resonance-guided and controlled radiotherapy. *Semin Radiat Oncol* 2014;24:196–9.
- [21] Fallone BG. The rotating biplanar linac-magnetic resonance imaging system. *Semin Radiat Oncol* 2014;24:200–2.
- [22] Liney GP, Jelen U, Byrne H, Dong B, Roberts TL, Kuncic Z, et al. Technical Note: the first live treatment on a 1.0 Tesla inline MRI-linac. *Med Phys* 2019. <https://doi.org/10.1002/mp.13556>.
- [23] Winkel D, Bol GH, Kroon PS, van Asselen B, Hackett SS, Werensteijn-Honingh AM, et al. Adaptive radiotherapy: the Elekta Unity MR-linac concept. *Clin Transl Radiat Oncol* 2019.
- [24] Raaijmakers AJ, Raaymakers BW, van der Meer S, Lagendijk JJ. Integrating a MRI scanner with a 6 MV radiotherapy accelerator: impact of the surface orientation on the entrance and exit dose due to the transverse magnetic field. *Phys Med Biol* 2007;52:929–39.
- [25] Verkooijen HM, Kerkmeijer LGW, Fuller CD, Huddart R, Favre-Finn C, Verheij M, et al. R-IDEAL: a framework for systematic clinical evaluation of technical innovations in radiation oncology. *Front Oncol* 2017;7:59.
- [26] Barentsz JO, Richenberg J, Clements R, Choyke P, Verma S, Villeirs G, et al. ESUR prostate MR guidelines 2012. *Eur Radiol* 2012;22:746–57.
- [27] Gladwish A, Pang G, Cheung P, D'Alimonte L, Deabreu A, Loblaw A. Prostatic displacement during extreme hypofractionated radiotherapy using volumetric modulated arc therapy (VMAT). *Radiat Oncol* 2014;9: 262–014-0262-y.
- [28] Woodings SJ, Bluemink JJ, de Vries JHW, Niatetski Y, van Veelen B, Schillings J, et al. Beam characterisation of the 1.5 T MRI-linac. *Phys Med Biol* 2018;63:085015–6560/aab566.
- [29] Elias E, Helou J, Zhang L, Cheung P, Deabreu A, D'Alimonte L, et al. Dosimetric and patient correlates of quality of life after prostate stereotactic ablative radiotherapy. *Radiother Oncol* 2014;112:83–8.
- [30] Pathmanathan AU, van As NJ, Kerkmeijer LGW, Christodouleas J, Lawton CAF, Vespri D, et al. Magnetic resonance imaging-guided adaptive radiation therapy: a “Game Changer” for prostate treatment? *Int J Radiat Oncol Biol Phys* 2018;100:361–73.
- [31] de Muinck Keizer DM, Pathmanathan AU, Andreychenko A, Kerkmeijer LGW, van der Voort van Zyp JRN, Tree AC, et al. Fiducial marker based intra-fraction motion assessment on cine-MR for MR-linac treatment of prostate cancer. *Phys Med Biol* 2019;64: 07NT02-6560/ab09a6.
- [32] Werensteijn-Honingh AM, Kroon PS, Winkel D, Aalbers EM, van Asselen B, Bol GH, et al. Feasibility of stereotactic radiotherapy using a 1.5 T MR-linac: multi-fraction treatment of pelvic lymph node oligometastases. *Radiother Oncol* 2019;134:50–4.
- [33] Bol GH, Lagendijk JJ, Raaymakers BW. Compensating for the impact of non-stationary spherical air cavities on IMRT dose delivery in transverse magnetic fields. *Phys Med Biol* 2015;60:755–68.
- [34] Uilkema S, van dH, Sonke J, Moreau M, van Triest B, Nijkamp J. 1.5 T transverse magnetic field in radiotherapy of rectal cancer: impact on the dose distribution. *Med Phys* 2015;42:7182–9.
- [35] Yang YM, Geurts M, Smilowitz JB, Sterpin E, Bednarz BP. Monte Carlo simulations of patient dose perturbations in rotational-type radiotherapy due to a transverse magnetic field: a tomotherapy investigation. *Med Phys* 2015;42:715–25.
- [36] Christiansen RL, Hansen CR, Dahlrot RH, Bertelsen AS, Hansen O, Brink C, et al. Plan quality for high-risk prostate cancer treated with high field magnetic resonance imaging guided radiotherapy. *Phys Imag Radiat Oncol* 2018;7:1–8.
- [37] van de Schoot AJAJ, van den Wollenberg W, Carbaat C, de Ruiter P, Nowee ME, Pos F, et al. Evaluation of plan quality in radiotherapy planning with an MR-linac. *Phys Imag Radiat Oncol* 2019;10:19–24.
- [38] Prior P, Chen X, Botros M, Paulson ES, Lawton C, Erickson B, et al. MRI-based IMRT planning for MR-linac: comparison between CT- and MRI-based plans for pancreatic and prostate cancers. *Phys Med Biol* 2016;61:3819–42.
- [39] Tseng C, Eppinga W, Seravalli E, Hackett S, Brand E, Ruschin M, et al. Dosimetric feasibility of the hybrid magnetic resonance imaging (MRI)-linac system (MRL) for brain metastases: the impact of the magnetic field. *Radiother Oncol* 2017;125:273–9.
- [40] Bainbridge HE, Menten MJ, Fast MF, Nill S, Oelfke U, McDonald F. Treating locally advanced lung cancer with a 1.5T MR-Linac – effects of the magnetic field and irradiation geometry on conventionally fractionated and isotoxic dose-escalated radiotherapy. *Radiother Oncol* 2017;125:280–5.
- [41] Menten MJ, Fast MF, Nill S, Kamerling CP, McDonald F, Oelfke U. Lung stereotactic body radiotherapy with an MR-linac – quantifying the impact of the magnetic field and real-time tumor tracking. *Radiother Oncol* 2016;119:461–6.
- [42] van Heijst TC, den Hartogh MD, Lagendijk JJ, van den Bongard HJ, van Asselen B. MR-guided breast radiotherapy: feasibility and magnetic-field impact on skin dose. *Phys Med Biol* 2013;58:5917–30.
- [43] Oborn BM, Ge Y, Hardcastle N, Metcalfe PE, Keall PJ. Dose enhancement in radiotherapy of small lung tumors using inline magnetic fields: a Monte Carlo based planning study. *Med Phys* 2016;43:368.